Bioorganic Chemistry 144 (2024) 107120

Contents lists available at ScienceDirect

Bioorganic Chemistry

journal homepage: www.elsevier.com/locate/bioorg

Design and synthesis of novel dithiazole carboxylic acid Derivatives: *In vivo* and *in silico* investigation of their Anti-Inflammatory and analgesic effects

Nazlı Turan Yücel [a], Abd Al Rahman Asfour [b], Asaf Evrim Evren [b,c,*], Cevşen Yazıcı [a], Ümmühan Kandemir [a,d], Ümide Demir Özkay [a], Özgür Devrim Can [a], Leyla Yurttaş [b]

[a] Department of Pharmacology, Faculty of Pharmacy, Anadolu University, Eskişehir 26100, Turkey
[b] Department of Pharmaceutical Chemistry, Faculty of Pharmacy, Anadolu University, Eskişehir 26100, Turkey
[c] Pharmacy Services, Vocational School of Health Services, Bilecik Seyh Edebali University, Bilecik 11100, Turkey
[d] Department of Medical Services and Techniques, Vocational School of Health Services, Bilecik Şeyh Edebali University, Bilecik 11100, Turkey

A B S T R A C T

Inflammation is a complex set of interactions that can occur in tissues as the body's defensive response to infections, trauma, allergens, or toxic compounds. Therefore, in almost all diseases, it can be observed because of primary or secondary reasons.

Since it is important to control and even eliminate the symptoms of inflammation in the treatment of many diseases, anti-inflammatory and analgesic drugs are always needed in the clinic. Therefore, the discovery of new anti-inflammatory/analgesic drugs with increased effectiveness and safer side effect profiles is among the popular topics of medicinal chemistry. Therefore, in this study, in order to synthesize and diversify new molecules, we focused on the N,*N*-dithiazole carboxylic acid core and linked it with the chalcone functional group.

The final eleven molecules were analyzed via HRMS, 1H NMR, and 13C NMR. The antinociceptive effects of the test compounds were examined by tail-clip, hot-plate, and formalin methods in mice, while their anti-inflammatory activities were investigated by carrageenan-induced inflammation tests in rats. The motor activities of the experimental animals were evaluated using an activity-meter device. Obtained findings revealed that none of the test compounds (10 mg/kg) were effective in the tail-clip and hot-plate tests. However, compounds 4b, 4c, 4f, 4 h, and 4 k in the serial shortened the paw-licking times of mice in the late phase of the formalin test indicating that these compounds had peripherally-mediated antinociceptive effects. The same compounds, moreover, showed potent anti-inflammatory effects by significantly reducing paw edema of rats in the inflammation tests. To provide an approach to pharmacological findings regarding possible mechanisms of action, the binding modes of the most active compounds were investigated by *in silico* approaches. The results of molecular docking studies indicated that the anti-inflammatory and analgesic activities of the compounds might be related to the inhibition of both COX-1 and COX-2 isoenzymes. Findings obtained from *in silico* studies showed that 4 k, which was chosen as a model for its analogs in the series, forms strong bindings to the basic residues (Arg120, Tyr355), side pocket loop area and deep hydrophobic regions of the enzyme. Moreover, results of the molecular dynamics simulation studies revealed that ligand-COX enzyme complexes are quite stable. Obtained results of *in vivo* and *in silico* studies are in harmony, and all together point out that compounds 4b, 4c, 4f, 4 h, and 4 k have significant anti-inflammatory and analgesic activities with good ADME profiles.

The potential of the derivatives, whose pharmacological activities were revealed for the first time in this study, as anti-inflammatory and analgesic drug candidates, needs to be evaluated through comprehensive clinical studies.

1. Introduction

The body's defensive reaction to infections, trauma, allergens, or toxic compounds manifests as a complex interplay of interactions within tissues, commonly referred to as inflammation. Serotonin, histamine, bradykinin and numerous endogenous mediators are abundant in inflammatory cells. Prostaglandins are among the main components that display and modulate inflammation-related cell and tissue responses [1]. The inflammatory process results in the development of redness, swelling, fever, pain, and other symptoms in the affected area [2]. Pain, one of these symptoms, is an aversive sensory and emotional experience that is crucial for the survival of an organism, providing immediate awareness of an existing or potential harm [3].

Although pain is the most common complaint of the majority of patients, it poses both diagnostic and therapeutic challenges for primary care units [4]. Today, there are many analgesic drugs used in the treatment of pain, non-steroidal anti-inflammatory drugs (NSAIDs) are the leading ones; however, mild or moderate side effects of these drugs, such as gastrointestinal problems, may limit their clinical use [5]. Considering the potency and side effect profiles of analgesic drugs used

* Corresponding author.
E-mail addresses: asafevrim.evren@bilecik.edu.tr, asafevrimevren@anadolu.edu.tr (A.E. Evren).

https://doi.org/10.1016/j.bioorg.2024.107120
Received 13 November 2023; Received in revised form 20 December 2023; Accepted 10 January 2024
Available online 12 January 2024

in the clinic, the discovery and development of new antinociceptive/anti-inflammatory drugs is of great importance.

NSAIDs such as flurbiprofen, piroxicam, indomethacin, acetylsalicylic acid, naproxen, and celecoxib possess a wide variety of heterocyclic ring systems in their structures. It has been demonstrated by *in vitro*, *in vivo* and *in silico* studies that they show their effects due to the presence of an acidic end connected to the aryl/heteroaryl structure in their main structure [6–11]. Either because of the ring itself in the aromatic structures such as phenyl, naphthalene, pyrazole, 10,10-dioxo-10λ6-thia-9-azabicyclo[4.4.0]deca-1,3,5-trien-7-one, pyridine, indole, or because of the acidic characters provided by of the carboxylic acid fragments such as acetic acid and propionic acid, and the sulphonic acid fragments like methyl sulphonyl and sulfonamides which are attached to this ring, these moieties have been reported to function as both hydrogen acceptor and donor at the protein active site [12–16]. This basic structure–activity relationship provides an insight into how currently available drugs and research compounds exert their inhibitory effects on prostaglandin synthesis.

Thiazole is an important ring structure that is reported to have broad pharmacological activities such as antimicrobial [17–19], antiviral [20,21] anticancer [22–24] neuroprotective [25–27] and hypoglycemic [28–30] effects. Moreover, thiazole derivatives have been reported for their anti-inflammatory and analgesic effects [31–33].

Based on the above-mentioned structure–activity relationships of NSAIDs and the pharmacological activity potential of thiazole ring system, in this study, thiazole-5-ylcarboxylic acid was processed as an aryl acid motif in the main structures of our test compounds. This structure was then linked to a thiazol-4-one ring, which is also a thiazole derivative, via a nitrogen atom. With this binding, the chalcone structure (C═C—CO), an important pharmacophore group whose anti-inflammatory and analgesic effects are frequently reported in the literature [34–37], was integrated into the double ring system. Finally, various chalcone analogues were obtained by derivation of interconnected thiazole rings with aldehydes. In this study, we aimed to examine the potential analgesic and anti-inflammatory activities of these eleven chalcone-thiazolone-thiazole carboxylic acid derivatives with some *in vivo* experiments and to investigate the relationships of effective derivatives with possible action sites *in silico* methods.

2. Materıals and methods

2.1. Chemistry

Chemicals used in the syntheses were purchased from either Merck Chemicals (Merck KGaA, Darmstadt, Germany) or Sigma-Aldrich Chemicals (Sigma-Aldrich Corp., St. Louis, MO, USA). Silica gel 60 F_{254} aluminum sheets obtained from Merck (Darmstadt, Germany) were used for observing the reactions and purities of the compounds by thin layer chromatography (TLC). The melting points of the synthesized compounds, presented as uncorrected, were recorded by MP90 digital melting point apparatus (Mettler Toledo, Ohio, USA). ^{1}H NMR and ^{13}C NMR spectra were recorded in DMSO-d_6 by a Bruker 400 MHz and 100 MHz digital FT-NMR spectrometer (Bruker Bioscience, Billerica, MA, USA), respectively, with splitting patterns designated as follows: s: singlet; d: doublet; t: triplet; m: multiplet. Coupling constants (J) were reported as Hertz. An LC/MS-IT-TOF system (Shimadzu, Kyoto, Japan) was used for high-resolution mass spectrometric (HRMS) studies. All spectra were shared in the supplementary file.

2.2. General synthesis of ethyl 2-amino-4-methylthiazole-5-carboxylate (1)

Thiourea (5 g, 0.065 mol) and 1.1 eq ethyl 2-chloroacetoacetate (9.99 ml, 0.060 mol) were added to a flask in the presence of ethanol as a solvent and at room temperature. The reaction was completed after 4 h, and it was confirmed by thin layer chromatography (TLC). The reaction mixture was filtered directly, and the material was left for a day to dry.

2.3. Synthesis of ethyl 2-(2-chloroacetamido)-4-methylthiazole-5-carboxylate (2)

In an ice bath, ethyl 2-amino-4-methylthiazole-5-carboxylate (9.6 g, 0.051 mol), (1 equivalent), triethylamine (TEA) (1.5 equivalent), and tetrahydrofuran (THF) as a solvent (200 ml), were added to the reaction flask. Acetyl chloride (4.92 ml, 0.043 mol), (1.2 equivalent) was diluted with THF solvent in the dropping funnel and then dropped into the reaction flask for approximately three hours. TLC was used to confirm that the reaction had ended, then we poured the mixture into a glass dish, the solvent, and TEA were evaporated under the fume hood, and distilled water was used to wash and filter the precipitated part, then left to dry [38].

2.4. Synthesis of ethyl 4-methyl-2-((4-oxo-4,5-dihydrothiazol-2-yl) amino)thiazole-5-carboxylate (3)

Ethyl 2-(2-chloroacetamido)-4-methylthiazole-5-carboxylate (8 g, 0.030 mol) was dissolved in ethanol and 1.2 equivalent of sodium thiocyanate (2.96 g, 0.036 mol) was added into the flask. After that, the mixture was stirred at reflux for 8 h. The end of the reaction was done by checking with TLC. The reaction solvent was evaporated, and the crude product was washed with water and filtered [39].

2.5. Synthesis of ethyl 4-methyl-2-((5-(substituted benzylidene)-4-oxo-4,5-dihydrothiazol-2-yl)amino)thiazole-5-carboxylic acid derivatives (4a-k)

A 2 N solution of sodium hydroxide was prepared in 50 ml of ethanol and put on the reflux to dissolve all the sodium hydroxide, then after it dissolves, we leave the solution to cool, then add the ethyl 4-methyl-2-((4-oxo-4,5-dihydrothiazol-2-yl)amino)thiazole-5-carboxylate (3) and stirred it for half an hour, then added the proper aldehyde derivative to it. The reaction was left for two hours until it was finished, and then we verified it with TLC. In the end, we filtered and left the material to dry. The raw products were recrystallized from ethanol.

2.6. (E/Z)-2-[(5-benzylidene-4-oxo-4,5-dihydrothiazol-2-yl)amino]-4-methylthiazole-5-carboxylic acid (4a)

2.6.1. ^{1}H NMR (400 MHz, DMSO-d_6, ppm) δ

2.45 (3H, s, CH_3), 7.33 (2H, m, J = 6.49 Hz, $Ph_{1,2}$), 7.46 (2H, t, J = 7.60 Hz, $Ph_{3,5}$), 7.55 (2H, d, J = 7.69 Hz, C<u>H</u>-Ph, Ph_4).

2.6.2. ^{13}C NMR (100 MHz) (DMSO-d_6) δ (ppm)

17.06 (<u>C</u>H_3), 119.42, 122.08, 123.91, 127.83, 129.35, 129.40, 136.16, 142.28, 150.23, 171.45, 173.52, 175.03, 180.82 (<u>C</u>O), 183,75 (<u>C</u>OOH).

2.6.3. HRMS (ESI) (m/z): [M + 1] $^{+}$

Calculated for C_{15} H_{11} N_3 O_3 S_2 346.0315.; found: 346.0316.

2.7. (E/Z)-4-methyl-2-[(5-(4-methylbenzylidene)-4-oxo-4,5-dihydrothiazol-2-yl)amino]thiazole-5-carboxylic acid (4b)

2.7.1. ^{1}H NMR (400 MHz, DMSO-d_6, ppm) δ

2.33 (3H, s, Ph-C<u>H</u>$_3$), 2.44 (3H, s, CH_3), 7.28 (2H, d, J = 7.87 Hz, $Ph_{3,5}$), 7.31 (1H, s, C<u>H</u>-Ph), 7.44 (2H, d, J = 7.85 Hz, $Ph_{1,2}$).

2.7.2. ^{13}C NMR (100 MHz) (DMSO-d_6) δ (ppm)

17.06 (<u>C</u>H_3), 21,41 (Ph-<u>C</u>H_3), 121.76, 124.00, 129.40, 129.96, 133.35, 135.78, 138.11, 146.52, 157.79, 166.49, 170.26, 171.57, 175.87 (<u>C</u>O), 178.19 (<u>C</u>OOH).

2.7.3. HRMS (ESI) (m/z): [M + 1] $^{+}$

Calculated C_{16} H_{13} N_3 O_3 S_2 360.0471.; found: 360.0475.

2.8. (E/Z)-4-methyl-2-[(5-(4-methoxybenzylidene)-4-oxo-4,5-dihydrothiazol-2-yl)amino]thiazole-5-carboxylic acid (4c)

2.8.1. ^{1}*H NMR (400 MHz, DMSO-*d_6*, ppm) δ*

2.45 (3H, s, C$\underline{H}_3$), 3.79 (3H, s, Ph-OC$\underline{H}_3$), 7.04 (2H, d, J = 7.38 Hz, $Ph_{3,5}$), 7.33 (1H, s, C$\underline{H}$-Ph), 7.50 (2H, d, J = 7.43 Hz, $Ph_{1,2}$).

2.8.2. ^{13}*C NMR (100 MHz) (DMSO-*d_6*) δ (ppm)*

17.10 (C$\underline{H}_3$), 55,75 (OC$\underline{H}_3$), 114.93, 124.12, 124.67, 127.42, 128.58, 131.02, 131.43, 133.83, 146.03, 148.77, 156.33, 159.61, 159.61, 184.68 (C$\underline{O}$), 192.13 (C$\underline{O}$OH).

2.8.3. HRMS (ESI) (m/z): [M + 1] $^{+}$

Calculated for C_{16} H_{13} N_3 O_4 S_2 376.0420.; found: 376.0425.

2.9. (E/Z)-4-methyl-2-[(5-(4-fluorobenzylidene)-4-oxo-4,5-dihydrothiazol-2-yl)amino]thiazole-5-carboxylic acid (4d)

2.9.1. ^{1}*H NMR (400 MHz, DMSO-*d_6*, ppm) δ*

2.45 (3H, s, CH_3), 7.31 (2H, d, J = 8.73 Hz, $Ph_{3,5}$), 7.36 (1H, s, CH-Ph), 7.59 (2H, q, J = 4.70 Hz, $Ph_{1,2}$).

2.9.2. ^{13}*C NMR (100 MHz) (DMSO-*d_6*) δ (ppm)*

23.06 ($\underline{C}H_3$), 97.74, 102.27, 126.74, 134.05, 135.68, 138.85, 143.58, 167.66, 172.76, 173.86, 177.58, 178.56, 181.28 ($\underline{C}$O), 187.75 ($\underline{C}$OOH).

2.9.3. HRMS (ESI) (m/z): [M + 1] $^{+}$

Calculated C_{15} H_{10} N_3 O_3 F S_2 364.0220.; found: 364.0222.

2.10. (E/Z)-4-methyl-2-[(5-(4-chlorobenzylidene)-4-oxo-4,5-dihydrothiazol-2-yl)amino]thiazole-5-carboxylic acid (4e)

2.10.1. ^{1}*H NMR (400 MHz, DMSO-*d_6*, ppm) δ*

2.45 (3H, s, CH_3), 7.34 (1H, s, C$\underline{H}$-Ph), 7.54 (4H, q, J = 9.02 Hz, Ph).

2.10.2. ^{13}*C NMR (100 MHz) (DMSO-*d_6*) δ (ppm)*

17.06 ($\underline{C}H_3$), 114.64, 122.53, 128.03, 129.38, 130.97, 132.70, 135.17, 141.85, 145.14, 149.37, 164.55, 168.09, 178.85 ($\underline{C}$O), 183.27 ($\underline{C}$OOH).

2.10.3. HRMS (ESI) (m/z): [M + 1] $^{+}$

Calculated C_{15} H_{10} N_3 O_3 S_2 Cl 379.9925.; found:379.9930.

2.11. (E/Z)-4-methyl-2-[(5-(4-nitrobenzylidene)-4-oxo-4,5-dihydrothiazol-2-yl)amino]thiazole-5-carboxylic acid (4f)

2.11.1. ^{1}*H NMR (400 MHz, DMSO-*d_6*, ppm) δ*

2.44 (3H, s, C$\underline{H}_3$), 7.46 (2H, d, J = 8.64 Hz, $Ph_{1,2}$), 7.80 (1H, s, C$\underline{H}$-Ph), 8.30 (2H, d, J = 8.64 Hz, $Ph_{3,5}$).

2.11.2. ^{13}*C NMR (100 MHz) (DMSO-*d_6*) δ (ppm)*

17.65 ($\underline{C}H_3$), 120.84, 124.67, 128.02, 130.22, 152.05, 153.36, 157.35, 163.20, 170.29, 171.16, 172.89, 179.49, 181.28 ($\underline{C}$O), 184,89 ($\underline{C}$OOH).

2.11.3. HRMS (ESI) (m/z): [M + 1] $^{+}$

Calculated C_{15} H_{10} N_4 O_5 S_2 391.0165.; found: 391.0170.

2.12. (E/Z)-4-methyl-2-[(5-(4-bromobenzylidene)-4-oxo-4,5-dihydrothiazol-2-yl)amino)thiazole-5-carboxylic acid (4 g)

2.12.1. ^{1}*H NMR (400 MHz, DMSO-*d_6*, ppm) δ*

2.45 (3H, s, C$\underline{H}_3$), 7.32 (1H, s, C$\underline{H}$-Ph), 7.50 (2H, d, J = 7.95 Hz, $Ph_{1,2}$), 7.65 (2H, d, J = 7.88 Hz, $Ph_{3,5}$).

2.12.2. ^{13}*C NMR (100 MHz) (DMSO-*d_6*) δ (ppm)*

17.01 ($\underline{C}H_3$), 123,98, 131.22, 132.27, 135.70, 139.65, 150.06, 154.31, 157.15, 161.48, 168.36, 175.56, 177.05, 181.39 ($\underline{C}$O), 187.57 ($\underline{C}$OOH).

2.12.3. HRMS (ESI) (m/z): [M + 1] $^{+}$

Calculated C_{15} H_{10} N_3 O_3 S_2 Br 423.9420.; found: 423.9419.

2.13. (E/Z)-4-methyl-2-[(5-(2-methylbenzylidene)-4-oxo-4,5-dihydrothiazol-2-yl)amino]thiazole-5-carboxylic acid (4 h)

2.13.1. ^{1}*H NMR (400 MHz, DMSO-*d_6*, ppm) δ*

2.37 (3H, s, C$\underline{H}_3$), 2.44 (3H, s, Ph-C$\underline{H}_3$), 7.26 (2H, m, J = 7.23 Hz, C$\underline{H}$-Ph, $Ph_{2,5}$), 7.53 (2H, t, J = 6.73 Hz, $Ph_{3,4}$).

2.13.2. ^{13}*C NMR (100 MHz) (DMSO-*d_6*) δ (ppm)*

17.05 ($\underline{C}H_3$), 20.10 (Ph-$\underline{C}H_3$), 121.16, 126.75, 127.75, 128.42, 130.94, 135.14, 135.55, 137.68, 144.15, 165,73, 173.92, 174.96, 181.05 ($\underline{C}$O), 188.02 ($\underline{C}$OOH).

2.13.3. HRMS (ESI) (m/z): [M + 1] $^{+}$

Calculated C_{16} H_{13} N_3 O_3 S_2 360.0471.; found: 360.0473.

2.14. (E/Z)-4-methyl-2-[(5-(2-fluorobenzylidene)-4-oxo-4,5-dihydrothiazol-2-yl)amino]thiazole-5-carboxylic acid (4i)

2.14.1. ^{1}*H NMR (400 MHz, DMSO-*d_6*, ppm) δ*

2.45 (3H, s, CH_3), 7.32 (3H, m, J = 9.15 Hz, C$\underline{H}$-Ph, $Ph_{2,5}$), 7.60 (2H, q, J = 4.66 Hz, $Ph_{3,4}$).

2.14.2. ^{13}*C NMR (100 MHz) (DMSO-*d_6*) δ (ppm)*

17.05 ($\underline{C}H_3$), 114.49, 116.48, 119.21, 130.51, 134.85, 136.92, 141.06, 147.36, 152.74, 158.94, 162.17, 165.28, 167.95 ($\underline{C}$O), 183.28 ($\underline{C}$OOH).

2.14.3. HRMS (ESI) (m/z): [M + 1] $^{+}$

Calculated C_{15} H_{10} N_3 O_3 F S_2 364.0220.; found: 364.0215.

2.15. (E/Z)-4-methyl-2-[(5-(2-chlorobenzylidene)-4-oxo-4,5-dihydrothiazol-2-yl)amino]thiazole-5-carboxylic acid (4j)

2.15.1. ^{1}*H NMR (400 MHz, DMSO-*d_6*, ppm) δ*

2.45 (3H, s, CH_3), 7.35 (1H, t, J = 7.62 Hz, Ph_3), 7.49 (1H, t, J = 7.57 Hz, Ph_4), 7.55 (1H, d, J = 7.96 Hz, Ph_2), 7.66 (2H, t, J = 10.98 Hz, C$\underline{H}$-Ph, Ph_5).

2.15.2. ^{13}*C NMR (100 MHz) (DMSO-*d_6*) δ (ppm)*

17.05 ($\underline{C}H_3$), 114.49, 116.48, 119.21, 130.51, 134.85, 136.92, 141.06, 147.36, 152.74, 158.94, 162,17, 165.28, 167.95 ($\underline{C}$O), 183.28 ($\underline{C}$OOH).

2.15.3. HRMS (ESI) (m/z): [M + 1] $^{+}$

Calculated C_{15} H_{10} N_3 O_3 S_2 Cl 379.9925.; found: 379.9920.

2.16. (E/Z)-4-methyl-2-[(5-(2-nitrobenzylidene)-4-oxo-4,5-dihydrothiazol-2-yl)amino]thiazole-5-carboxylic acid (4 k)

2.16.1. ^{1}*H NMR (400 MHz, DMSO-*d_6*, ppm) δ*

2.50 (3H, s, CH_3), 7.61 (1H, s, C$\underline{H}$-Ph), 7.83 (2H, q, J = 5.46 Hz,

$Ph_{3,4}$), 8.07 (2H, d, J = 8.12 Hz, $Ph_{2,5}$).

2.16.2. ^{13}C NMR (100 MHz) (DMSO-d_6) δ (ppm)

17.79 ($\underline{C}H_3$), 110.48, 115.87, 119.99, 129.47, 137.77, 149.08, 157.02, 163.25, 167.47, 169.17, 177.33, 182.78 ($\underline{C}O$), 200.77 ($\underline{C}OOH$).

2.16.3. HRMS (ESI) (m/z): [M + 1] $^+$

Calculated $C_{15}H_{10}N_4O_5S_2$ 391.0165.; found: 391.0181.

3. Pharmacology

3.1. Animals

Nociception and motor activity tests and gastric evaluations were performed using adult male BALB/c mice (30–35 g), and paw edema tests were performed using adult male Sprague Dawley rats (200–250 g). All animals were housed under controlled environmental conditions (temperature of 24 ± 1 °C, 12-hour light/dark cycle) and maintained with *ad libi*tum access to water and pellet diet. The experimental procedure has been approved by the Local Ethical Committee on Animal Experimentation of Anadolu University, Eskişehir, Turkey. (Ethical approval number: 2023–29 and date: 14.06.2023).

3.2. Administrations of the test compounds

Test compounds were dissolved in 0.5 % (w/v) carboxymethyl cellulose solution and administered intraperitoneally to animals at a dose of 10 mg/kg [40]. Experiments were carried out 30 min after the treatments.

Reference drug, morphine sulfate (10 mg/kg, i.p.) [41] was used for analgesia experiments in mice, while diclofenac sodium (20 mg/kg, i.p.) [42] was used for carrageenan-induced paw edema tests in rats. The control groups received 0.5 % (w/v) carboxymethyl cellulose solution as the solvent for the test compounds.

3.3. Motor activity tests

3.3.1. Activity test

An activity-meter device (Commat, MayAMS02, Ankara, Türkiye) was used to measure the motor activities of animals. In this test, the total activities of the mice and the distance they traveled on the device were recorded for 4 min [43].

3.4. Nociceptive tests

3.4.1. Hot-plate test

A hot-plate test was used to evaluate the responses of the animals against thermal nociceptive stimuli (Ugo-Basile, 7280, Verase, Italy). In this experiment, the temperature setting of the heated surface of the hot-plate apparatus was adjusted to 55 ± 1.0 °C, and the onset of the foot licking and/or jumping over the plate behaviors of animals were recorded after they had been exposed to the painful stimulus.

Prior to the experiment, the animals were checked for their susceptibility and those that responded within 15 s were chosen for the experiments. Then they were individually placed on the metal plate of the device both before and after the drug administrations, and their pain thresholds were assessed. During these trials, the animals were not exposed to the stimuli for more than 30 s for not to cause any permanent harm to the paws [44,45].

3.4.2. Tail-clip test

A tail-clip test was used to evaluate the responses of the animals against mechanical nociceptive stimuli. In this test, a clamp was attached to the tails of the mice and the time when animals turned and bit the clamp was measured with a stopwatch. The increase in the reaction times of the animals was accepted as a parameter for the antinociceptive effect [45,46].

A sensitivity assessment test was performed prior to the experiments, and animals that did not respond to the clamp within 10 s were excluded from the experiment. In the test session, pain thresholds of the animals were individually evaluated before and after the drug administrations. The painful stimulus was applied for a maximum of 10 s to prevent the tail from being damaged during the tests [44].

The reaction times measured both in hot-plate and tail-clip tests were given as the percentage of the maximum possible effect (MPE), which was calculated as in the following:

$$\text{MPE}\,\% = \frac{(\text{postdrug latency} - \text{predrug latency})}{(\text{cutoff time} - \text{predrug latency})} x100$$

3.4.3. Formalin test

Formalin-induced nociception test was used to evaluate inflammatory pain responses in experimental animals [47]. For this purpose, 25 µl 5 % formalin solution was injected into the intraplantar region of the right hind paws of mice. Then each animal was observed for 30 min and the duration of the licking/biting behaviors for the treated paw was recorded. 0–5 min following the formalin injection was considered as the early phase, and the time between 15–30 min was defined as the late phase [1,48]. The reduction in the paw-licking times of the animals was acknowledged as a measure of the antinociceptive effect.

3.5. Inflammation tests

3.5.1. λ-carrageenan-induced paw edema test

An acute inflammation model of carrageenan-induced paw edema is frequently used to assess the anti-inflammatory effects of drugs and/or test compounds [49]. This procedure was performed by a 0.1 ml of λ-carrageenan (1 % w/v) injection in the subplantar region of the right hind paws of rats. A plethysmometer device (Ugo Basile, 37140, Italy) was used to measure the volume of the paws immediately before the carrageenan injection, and at 0.5, 1, 2, 3, and 4 h following the injection [49]. The % increase in paw volume was determined as in the following [50]:

$$\text{The swelling rate} = \frac{(\text{Paw volume at each time point} - \text{the initial paw volume})}{\text{The initial paw volume}} x100$$

Investigators were blinded to group allocation throughout the *in vivo* experiments, outcome evaluation, and data analyses.

3.6. Statistical analysis

Data from eight animals in each experimental group were analyzed using Graphpad Prism ver 8.4.3 package program (GraphPad Software, San Diego, CA, USA). Variables were first investigated for normality and homogeneity of variance using Shapiro–Wilk and Levene tests, respectively. Significant differences between groups were determined by one-way analysis of variance (ANOVA), followed by Tukey HSD tests for multiple comparisons. A value of $p < 0.05$ was considered significant and results were given as mean ± standard error of the mean.

3.7. In silico analyzes

To understand the binding mode, also to clarify the structure–activity relationship (SAR) of the active compounds, exactly the same procedure for molecular docking, and molecular dynamics studies were applied as in our previous study [51] and evaluated similarly as in previous studies, too [17,18,23,52–54].

3.8. Molecular docking

The COX-1 and COX-2 X-ray crystal structures (PDB ID: 2OYU and 6COX, respectively) were retrieved from the Protein Data Bank server

(https://www.pdb.org, accessed May 01, 2021). Schrödinger's Maestro [55] interface and its applications (LigPrep module [56], Glide module [57]) were used for the molecular docking study. Docking runs were performed in standard precision docking mode (SP). This procedure was applied previously [51,58].

3.9. Molecular dynamics simulation (MDS)

MDS method is a useful technology to predict the time-dependent stability of the systems such as apoproteins, ligand-enzyme or ligand receptor, *etc*. In this study, the best poses, obtained from the docking studies, of 4 k-COX-1 and **4 k**-COX-2 complexes were investigated through 100 ns. Desmond's application of Schrodinger's Maestro [59] was used to achieve MDS according to previous methods [51,58]. The neutralization of the system was achieved using Na^+ and Cl^- ions to provide a final salt concentration of 0.15 M in order to simulate physiological concentration of monovalent ions. Constant temperature (310.55 K) and pressure (1.01325 bar) were employed with NPT (constant number of particles, pressure, and temperature) as ensemble class. RESPA integrator was used in order to integrate the equations of motion. NH thermostats [36] were used to keep the constant simulation temperature, and the MTK method was applied to control the pressure. Long-range electrostatic interactions were calculated by pmE method. The cutoff for van der Waals and short-range electrostatic interactions was set at 9.0 Å. The equilibration of the system was performed with the default protocol provided in Desmond, which consists of a series of restrained minimizations and molecular dynamics simulations used to slowly relax the system.

4. Results and discussion

4.1. Chemistry

The compounds **4a–4 k** were synthesized as summarized in Fig. 1. The compounds were synthesized in the laboratory through a four-step process. Firstly, the thiazole ring was closed by reacting ethyl 2-chloroacetoacetate with thiourea in the presence of ethanol as a protic solvent, resulting in the formation of ethyl 2-amino-4-methylthiazole-5-carboxylate. In the second step, the intermediate product was acetylated by treating it with chloro acetylchloride in THF solvent, leading to the formation of ethyl 2-(2-chloroacetamido)-4-methylthiazole-5-carboxylate. The third step involved the closure of the thiazole ring by reacting the compound with sodium thiocyanate in ethanol solvent under heat. In the fourth step, a sodium hydroxide solution was added like the initial step, followed by the addition of the aldehyde derivative to obtain the final chalcone-thiazole carboxylic acid derivatives.

In the ^{1}H NMR spectra, the observed peaks align with their estimated areas. Analysis revealed several consistent features across the compounds. All compounds displayed methyl (CH_3) groups, typically appearing as singlets within the chemical shift range of 2.44–2.50 ppm. Aromatic protons were present in most compounds, exhibiting a broad range of chemical shifts from 7.04 to 8.30 ppm, accompanied by various multiplicities such as doublets, triplets, quartets, and multiplets. Another recurring signal observed was aromatic hydrogen protons, typically appearing between 7.31 and 7.66 ppm. Additionally, the presence of $Ph_{1,2}$ signals was common, observed within the chemical shift range of 7.33–7.55 ppm and exhibiting doublet or multiplet patterns.

The ^{13}C NMR spectra of the compounds (**4a**) to (**4 k**) revealed distinct peaks at their estimated areas, providing valuable information about their chemical composition. Peaks in the range of 175–208.06 ppm were observed for all compounds, suggesting the presence of a carbon of carboxylic acid group (COOH). The other common group for all compounds, 4-$\underline{C}H_3$ thiazole, its methyl carbon was observed between 17.01 and 17.79 ppm. Overall, the ^{13}C NMR spectra provided valuable insights into the structural and chemical characteristics of these compounds.

The mass spectra (ESI-MS) of the compound's [M + H] peaks agreed with their predicted molecular formula **4a–4 k.**

4.2. ADME parameters

The SwissADME online tool was utilized to perform a comprehensive evaluation of the physicochemical properties, pharmacokinetics, and medicinal chemistry information of the test compounds (Table 1). The HBA values of the 11 compounds ranged from 5 to 7, and the HBD values were 2 for all compounds, showing their potential for hydrogen bonding. The TPSA values for all the compounds were between 145 and 191 $Å^2$, which suggests their capability for interacting with biological targets.

The Log P o/w and Log P S values of the compounds ranged from 2.6 to 3.22 and −4.31 to −5.16, respectively, indicating their lipophilicity and water solubility abilities, respectively. The compounds exhibited low GIA values, which suggests that they are low efficiently absorbed through the gastrointestinal tract. The Log Kp values of the compounds ranged from −6.35 to −5.72, illustrating their ability to penetrate the skin. The RoF values for the compounds ranged from 0 to 2, which implies that the compounds are likely to be cleared through the kidneys,

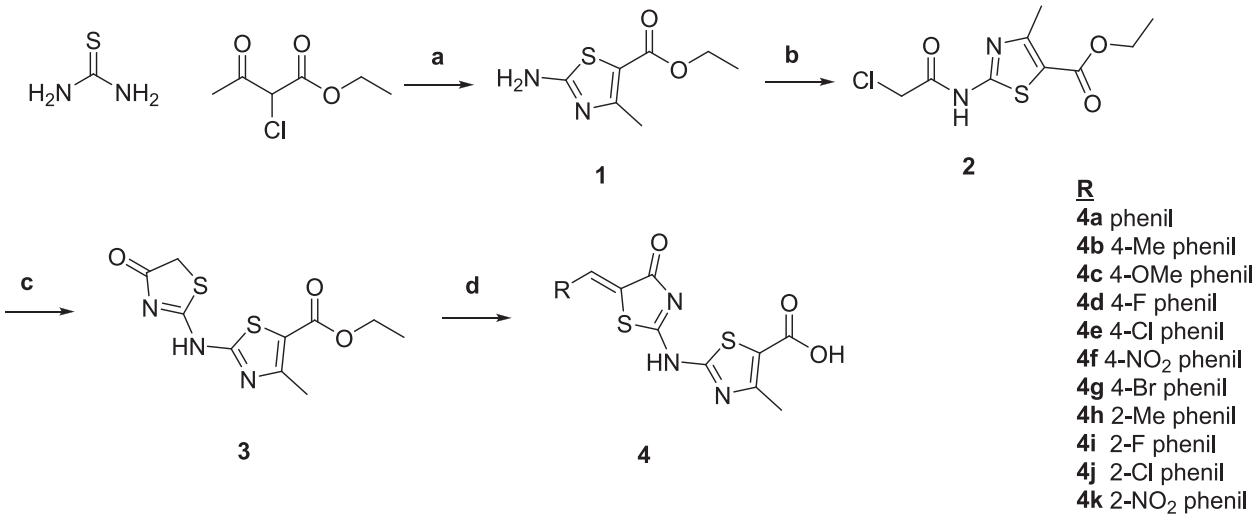

Fig. 1. Synthesis route for all molecules.

Table 1
Some important features* of the synthesized compounds.

Physicochemical Properties					Pharmacokinetics		Medicinal Chemistry	
HBA	HBD	TPSA	Log $P_{o/w}$	Log P_s	GIA	Log Kp	RoF (V)	SA
5	2	145.19	2.6	−4.24	Low	−5.96	0	3.57
5	2	145.19	2.91	−4.55	Low	−5.78	2	3.68
6	2	154.42	2.6	−4.32	Low	−6.15	1	3.62
6	2	145.19	2.91	−4.4	Low	−6	2	3.53
5	2	145.19	3.13	−4.84	Low	−5.72	2	3.55
7	2	191.01	1.83	−4.31	Low	−6.35	1	3.59
5	2	145.19	3.22	−5.16	Low	−5.94	2	3.56
5	2	145.19	2.91	−4.55	Low	−5.78	2	3.7
6	2	145.19	2.89	−4.4	Low	−6	2	3.57
5	2	145.19	3.19	−4.84	Low	−5.72	2	3.58
7	2	191.01	1.85	−4.31	Low	−6.35	1	3.68

* **HBA:** H-bond acceptor, **HBD:** H-bond donor, **TPSA:** Topologic polar surface area ($A^{\circ 2}$) **Log Po/w:** Consensus Log Po/w (Average of all five predictions), **Log S (ESOL):** Water Solubility, **GIA:** Gastrointestinal absorption, **Log Kp:** skin permeation (cm/s) **RoF (V):** Rule of Five (number of violation).

the SA values of the compounds ranged from 3.53 to 3.7, indicating their ease of synthesis. Additionally, Lipinski's rule was satisfied for all the compounds, indicating that the compounds are proper to use orally, however, their bioavailability rates are low due to GIS absorption. Furthermore, the analysis revealed that the compounds possess pharmacophore or drug-like features that adhere to and fulfill Lipinski's rule, with all attributes being within acceptable ranges. As a result, predictions reported that final compounds are promising candidates for further drug development.

4.3. Pharmacology

The next step of this study was to investigate the potential antinociceptive and anti-inflammatory effects of these novel thiazole carboxylic acid derivatives. However, before antinociceptive effect tests, motor activity studies were performed to evaluate whether the compounds would cause false positive responses in experimental animals. Fig. 2 shows the effects of test compounds (10 mg/kg) on the (A) total activity [$F(11, 84) = 0.52$; $p > 0.05$] and (B) distance [$F(11, 84) = 0.57$; $p > 0.05$] values of the mice in the activity-meter measurements.

The results of the ANOVA analysis revealed that none of the test compounds caused a significant change on the total activity numbers and total distance values recorded in the activity meter test of the mice. These findings are important in terms of showing that the findings obtained from tests evaluating antinociceptive activity are specific.

After it was revealed that the test compounds did not change the motor performance of the experimental animals, nociceptive tests were started. The potential antinociceptive efficacy of the test compounds was evaluated by hot-plate, tail-clip and formalin tests. The effect of test compounds on MPE % values calculated in hot-plate tests is presented in Fig. 3 [$F(12, 91) = 9.28$; $p < 0.001$].

The findings revealed that morphine used as the reference drug increased the MPE% values calculated for the hot-plate test compared to the control group ($p < 0.001$), but none of the test compounds changed these values in a statistically significant way. The results obtained showed that the test compounds had no antinociceptive activity in the hot-plate test and were ineffective on the supraspinal mechanisms that process nociceptive stimuli [60].

Fig. 4 displays the effect of test compounds on MPE % values calculated in tail-clip tests [$F(12, 91) = 17.05$; $p < 0.001$].

Results from the tail-clip test revealed that, similar to the hot-plate test, morphine significantly increased the MPE % values compared to the control group ($p < 0.001$), but the test compounds were ineffective. In other words, the tested compounds do not affect the spinal mechanisms that process nociceptive stimuli, nor do they affect the supraspinal mechanisms [60,61].

Fig. 5 shows the effects of test compounds on mice' paw licking times in the early **(A)** [$F(12, 91) = 6.75$; $p < 0.001$] and late **(B)** [$F(12, 91) = 9.49$; $p < 0.001$] phases of the formalin tests.

The formalin test is a frequently used method to examine the central and/or peripheral antinociceptive effects of drugs or test agents. The basis of the test is that intraplantar administration of formalin solution causes a biphasic nociceptive reaction in rodents that is suppressed by analgesic drugs. In the test, the first phase (0–5 min), which begins immediately after the formalin injection, is known as the "early" or "neurogenic" phase. The neurogenic phase is considered to be associated

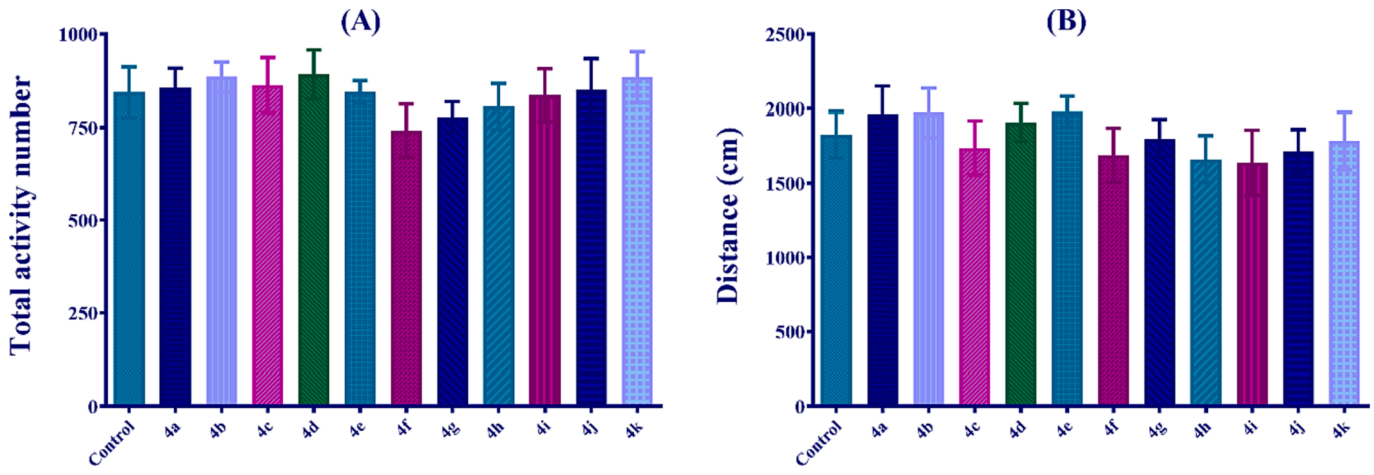

Fig. 2. The effects of control solution and test compounds (10 mg/kg) administrations on the (**A**) total activity number and (**B**) total distance values of animals in the activity-meter measurements. One-way ANOVA followed by Tukey HSD multiple comparison test, n = 8.

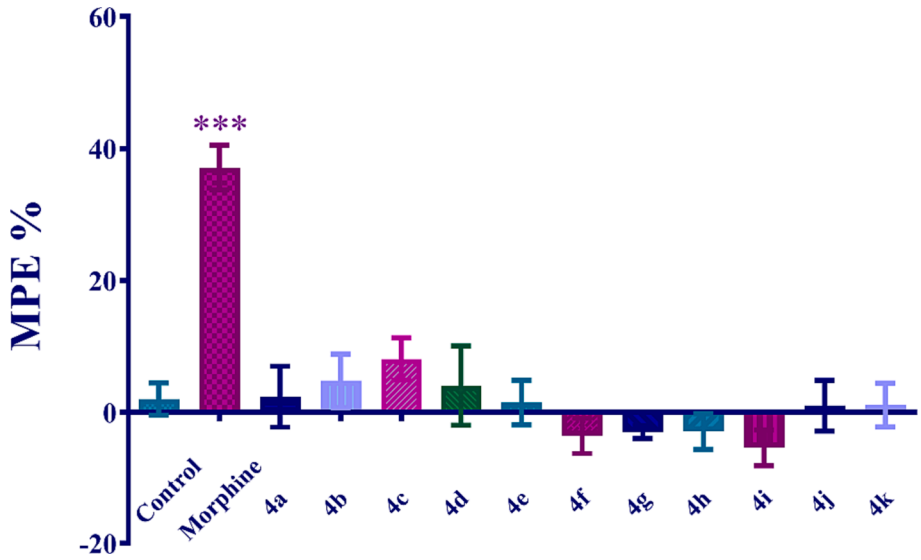

Fig. 3. The effects of control solution, morpine sulphate (10 mg/kg) and test compounds (10 mg/kg) administrations on the MPE % values of mice calculated in the hot-plate tests. Significance against control group ***$p < 0.001$ One-way ANOVA followed by Tukey HSD multiple comparison test, $n = 8$.

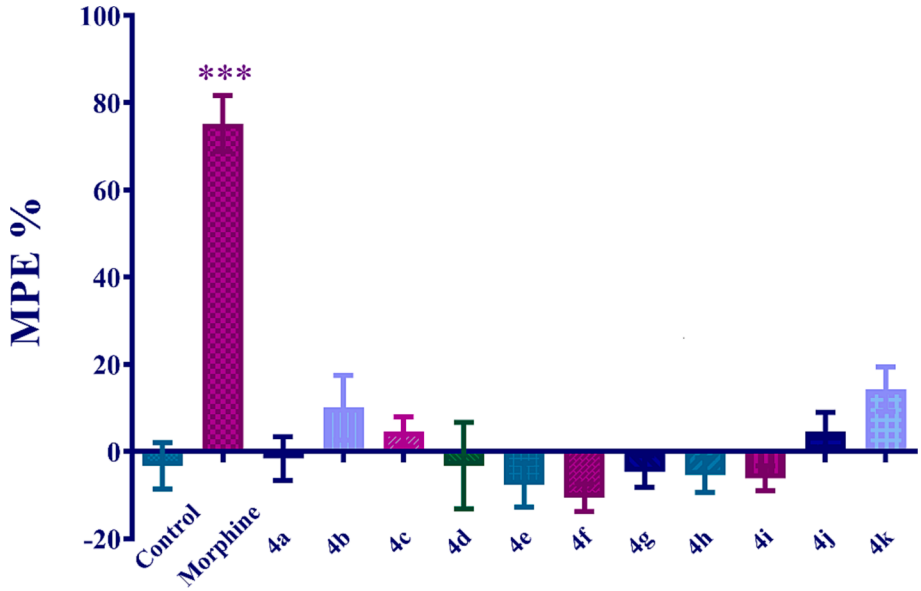

Fig. 4. The effects of control solution, morpine sulphate (10 mg/kg) and test compounds (10 mg/kg) administrations on the MPE % values of mice calculated in the tail-clip tests. Significance against control group ***$p < 0.001$. One-way ANOVA followed by Tukey HSD multiple comparison test, $n = 8$.

with central pain carried by the C fibers in particular, due to the direct stimulation of nociceptors during this period. The second phase of the test (15–30 min) is considered as the "inflammatory phase". In this phase, various mediators such as histamine, prostaglandins, serotonin and bradykinin are released from peripheral tissues and functional changes are observed in the spinal dorsal horn. It has been shown that centrally acting analgesic drugs inhibit both phases of the formalin test, while peripherally acting analgesic drugs inhibit only the late phase of this test [62–65].

In this study, the results of the statistical analysis presented that our thiazole carboxylic acid analogs did not cause any significant change in the paw licking times of the mice in the first phase of the formalin test (5**A**). Therefore, it can be said that none of the test compounds have a centrally-mediated antinociceptive effect; this supports the results of the hot-plate and tail-clip tests performed in this study. On the other hand, compounds **4b**, **4c**, **4f**, **4 h** and **4 k** significantly inhibited the second phase of the formalin test (**5B**). These effects of the mentioned compounds in the second phase of the test indicate the presence of a peripherally-mediated antinociceptive effect.

Within the scope of this study, the anti-inflammatory activities of the test compounds were also investigated in light of the findings obtained from the formalin tests. Carrageenan-induced paw edema test was performed to investigate potential anti-inflammatory activity.

Fig. 6 shows the effects of test compounds (10 mg/kg) and diclofenac (20 mg/kg) administrations on the paw swelling rates (%) of rats, measured 0.5 hr (A) [$F(12, 91) = 4.34$; $p < 0.001$], 1 hr (B) [$F(12, 91) = 5.65$; $p < 0.001$], 2 hrs (C) [$F(12, 91) = 5.91$; $p < 0.001$], 3 hrs (D) [$F(12, 91) = 7.75$; $p < 0.001$] and 4 hrs (E) [$F(12, 91) = 6.27$; $p < 0.001$] after the injection of carrageenan in the inflammation tests.

In this study, multiple comparison analyses revealed that test compounds **4b**, **4c**, **4f**, **4 h,** and **4 k** significantly reduced the paw edema rates of rats at 1, 2, and 3 h after the carrageenan injections compared

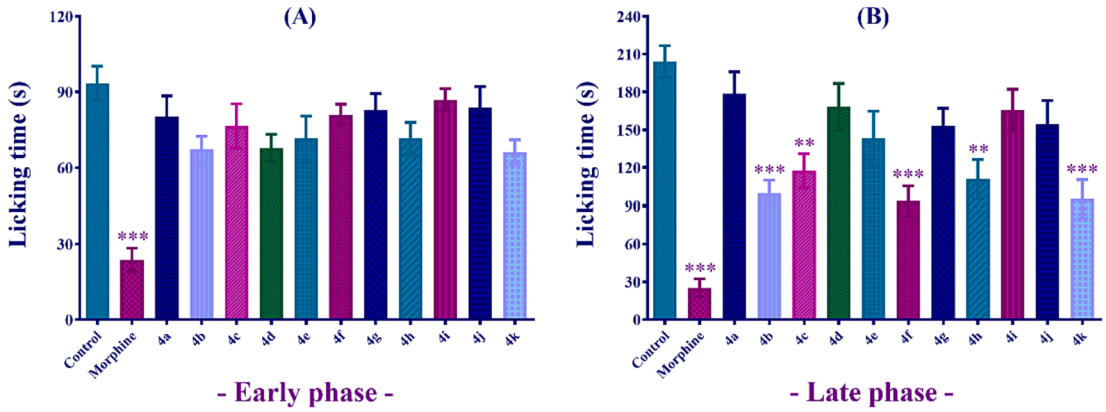

Fig. 5. The effects of control solution, morpine sulphate (10 mg/kg) and test compounds (10 mg/kg) administrations on the mice' paw licking times in the **(A)** early and **(B)** late phases of formalin tests. Significance against control group **p < 0.01; ***p < 0.001. One-way ANOVA followed by Tukey HSD multiple comparison test, n = 8.

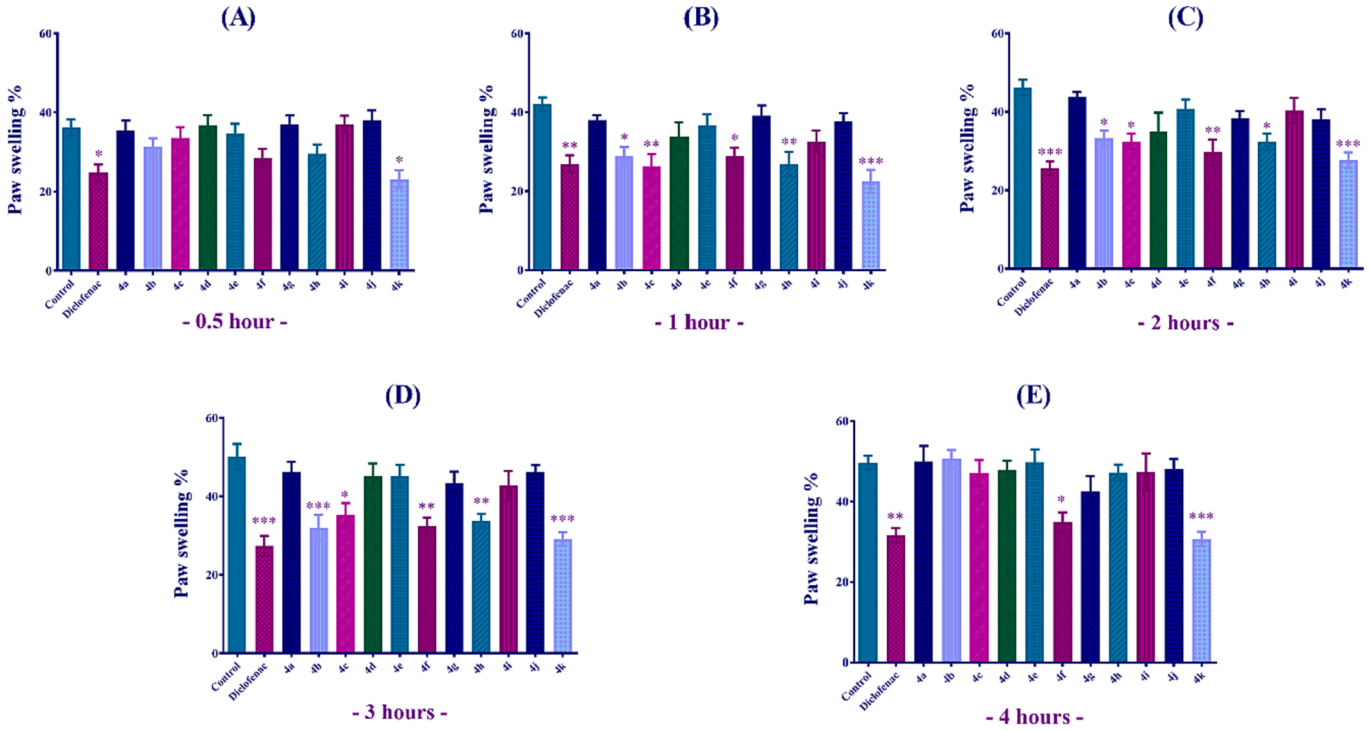

Fig. 6. The effects of control solution, diclofenac sodium (20 mg/kg) and test compounds (10 mg/kg) administrations on the paw swelling rates of rats 0.5 hr **(A),** 1 hr **(B)**, 2 hrs **(C)**, 3 hrs **(D)** and 4 hrs **(E)** after the carrageenan injection in the inflammation tests. Significance against control group *p < 0.05; **p < 0.01; ***p < 0.001. One-way ANOVA followed by Tukey HSD multiple comparison test, n = 8.

with the corresponding control groups. Obtained data indicate that these compounds have anti-inflammatory effects at 10 mg/kg dose. It was observed that the edema-reducing effect of compound **4 k** started at 30 min and continued throughout the entire test period. This compound showed an anti-inflammatory activity comparable to the reference drug diclofenac (20 mg/kg) at all-time points. In addition, the effect of compound **4f** was prolonged up to 4 h, unlike compounds **4b**, **4c,** and **4 h**. Intraplantar injection of carrageenan triggers an inflammatory process with extravasation of cells and proteins and causes edema formation with the effect of proinflammatory mediators [50,66]. In the carrageenan-induced paw edema test, the development of edema is a biphasic event. The initial phase (approximately 1 h) is the non-phagocytic edema phase, predominantly attributed to the release of mediators such as histamine, bradykinin, and serotonin. The second/late phase (after 2 h) is a rapid swelling period, which is associated with increased production of prostaglandins, oxygen-derived free radicals, and quinine-like compounds. Therefore, it can be suggested that compounds **4b**, **4c**, **4f**, **4 h** and **4 k** exert their pharmacological activities by inhibiting both phases of the carrageenan-induced inflammatory response, and their anti-inflammatory effects are mediated by the suppression of various mediators that play critical roles in the inflammation process.

The findings obtained at the end of the pharmacological studies revealed that our specifically designed and synthesized chalcone-thiazolone-thiazole carboxylic acid derivatives showed analgesic and anti-inflammatory effects as hypothesized at the beginning of the study.

4.4. In silico analysis results

In this study, as mentioned in the introduction section, the

pharmacophore structure of final compounds is similar to NSAI drugs (aryl carboxylic acid residue), and also, their effect is observed on the peripheral pathway, not on the central nervous system, and finally, the *in vivo* tests suggested that they have both analgesic and anti-inflammatory activity, pointing out that the mechanism of action is the similar to the pathway of action of NSAI drugs. So, firstly, docking studies were performed and possible binding modes were evaluated according to the best docking pose for each active compounds. The best poses of potential COX enzyme (COX-1 or COX-2) inhibitors were displayed in Fig. 7 and Fig. 8, respectively. According to Fig. 7, active compounds jointly interacted with Arg120 (H-bond) and Ser516 (H-bond). All active compounds formed an H-bond with Ser353 residue via nitrogen of *N,N*-dithiazole amine while compound **4 k** did not, but it formed an π-π stacking with Tyr355 instead of Ser353. Only one compound, **4b**, interacted with polar amino acids (Arg120, Ser353, and Ser516) of ligand-binding canal in the COX-1 enzyme, and moreover, all compounds localized at polar pocket of the enzyme by similar shape. The difference in binding mode of them is probably related to the hydrophobic side of the enzyme. It seems that substitution type changes the binding to hydrophobic residues but does not affect the conformational stability of the ligand. However, thiazole carboxylic acid moieties of **4j** (2-fluorophenyl) and **4 k** (2-nitrophenyl) rotated oppositely 180° rather than other active compounds, resulting in different contact with one residue. **4 k** interacted with Phe518 (π-π stacking) when **4j** contacted with Arg120 (salt bridge, and extra one H-bond).

According to Fig. 8, all active compounds have two common interactions that were observed as H-bonds with Arg120 and Tyr355 residues. In addition to that, only fluor substitutions (**4d** and **4j**) constituted a salt bridge with Arg120. On the other hand, except 4-fluoro and 2-fluoro derivatives (**4d** and **4j**), compound **4 g** (with its carboxylic acid moiety) and other active compounds **4b**, **4c**, **4i**, and **4 k** (with their thiazole nitrogen) formed an H-bond with Hie90 residue. Additionally, except **4 g**, actives compounds formed an H-bond with Phe518. Both residues are in additional side pocket of COX-2 enzyme, thus, forming with those residues are stabilized enzyme and so increased inhibitory effect. The other important binding residues were Tyr385, Met522, Val523, and Ser530 in addition to the above. As a result, all these interactions were observed similarly between ligands and COX-1 enzyme, therefore, we suggested that there is no meaningful selectivity index against COX isoforms.

After determining the best poses of the compounds, the most powerful inhibitor analog, **4 k**, was chosen as a pattern to observe ligand–protein complex stability and its behavior during environmental changes. The stability plots of MDS (**A**, **B**, and **C** in the related figure), its

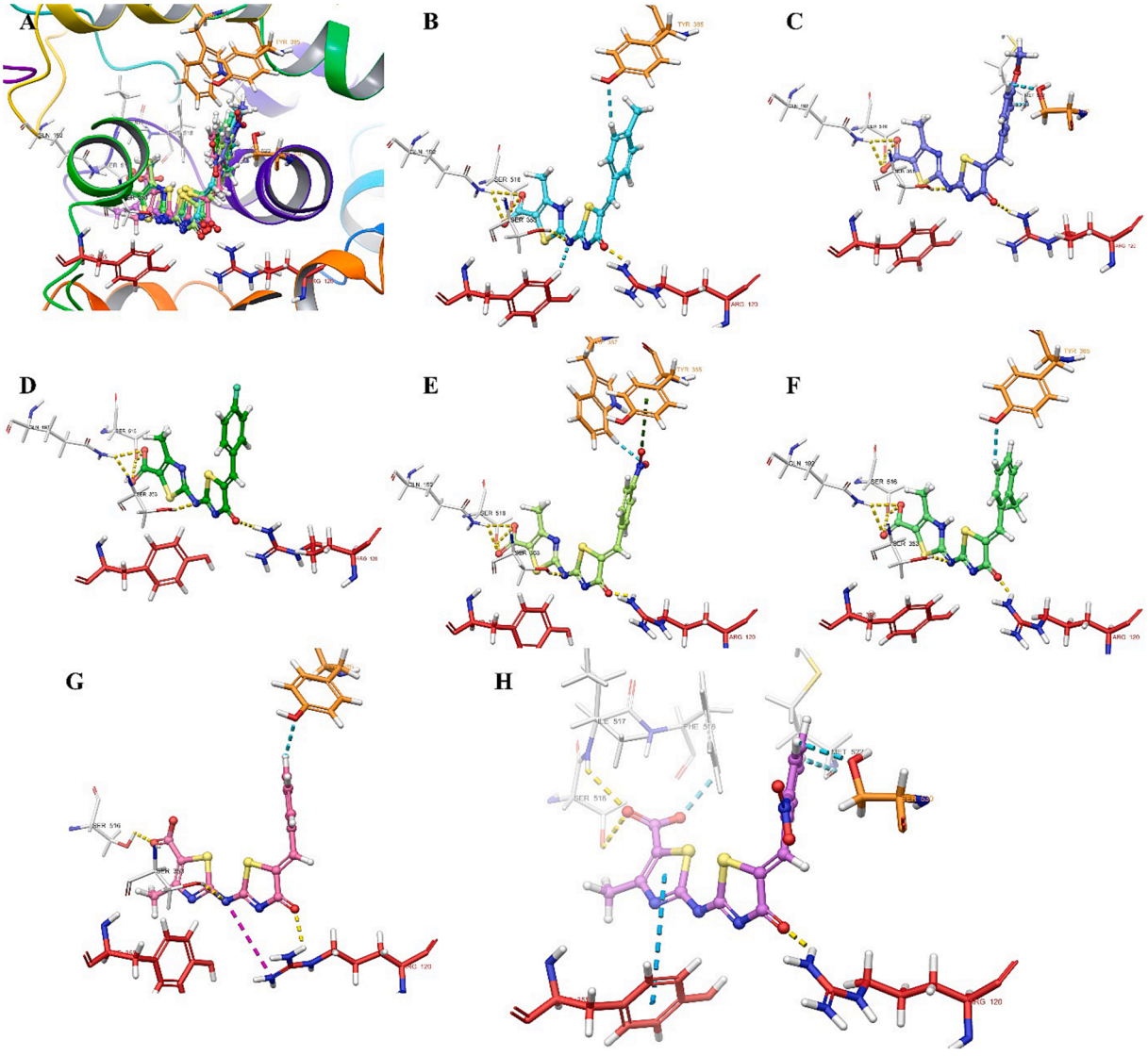

Fig. 7. The docking poses of the active compounds. **A:** Superimposition of active compounds inside the active pocket of the COX-1 enzyme. 3D poses of **B: 4b**, **C: 4c**, **D: 4d**, **E: 4 g**, **F: 4i**, **G: 4j**, **H: 4 k**.

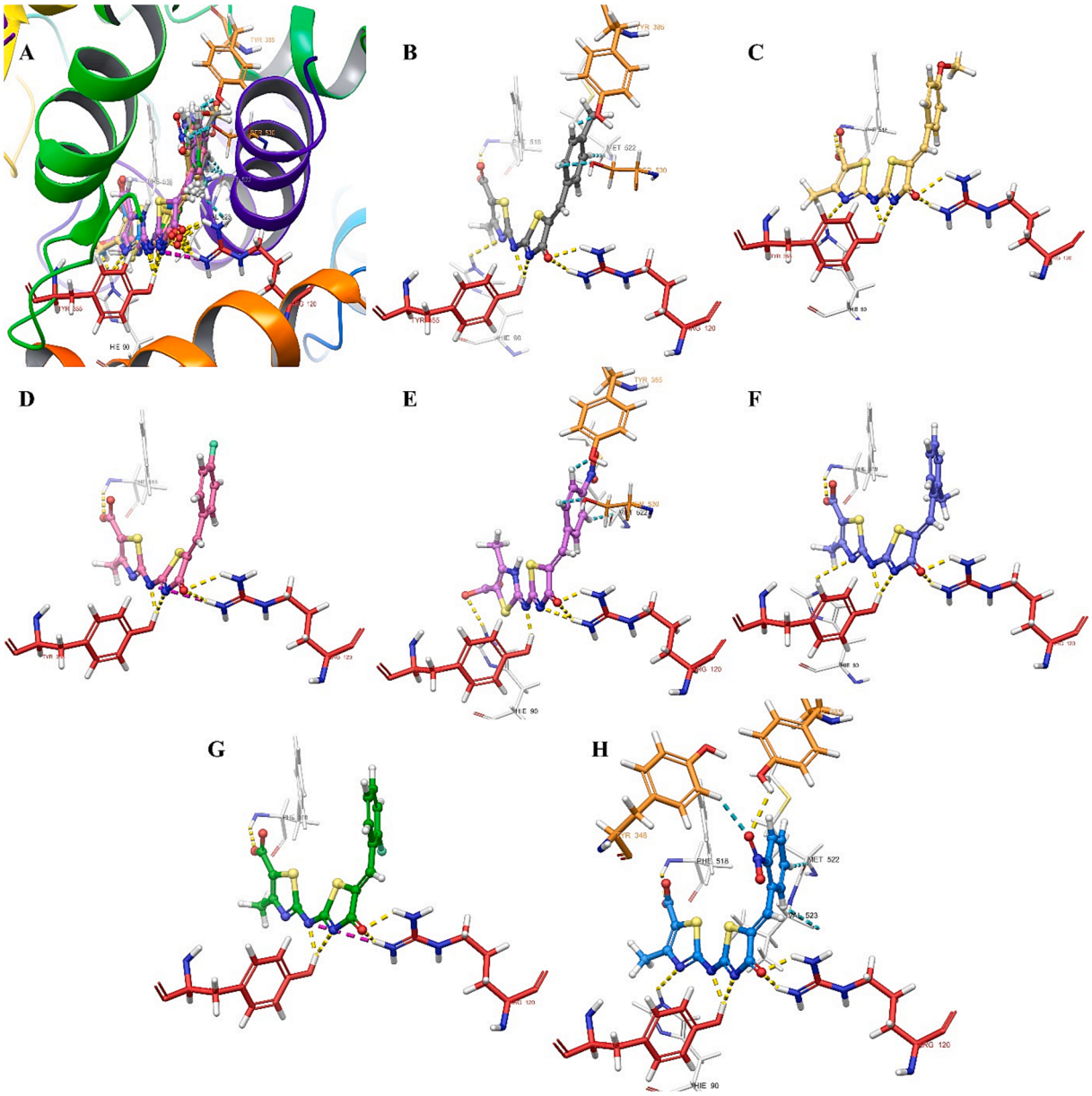

Fig. 8. The docking poses of the active compounds. **A:** Superimposition of active compounds inside the active pocket of the COX-2 enzyme. 3D poses of **B: 4b C: 4c**, **D: 4d**, **E: 4 g**, **F: 4i**, **G: 4j**, **H: 4 k**.

data plots (**E** and **D** in the related figure), and the interactions are shown in **videos (1 and 2)**, Fig. 9, and Fig. 10.

According to **A**, **B,** and **C** of Fig. 9 and Fig. 10, Rg, RMSD (protein, protein–ligand, and ligand–ligand), and RMSF values were found in an acceptable range for both complex according to previous studies [17,18,23,24,53]. For both complexes, Rg values did not show any drastic changes, RMSD values of C_α were calculated 2.34 Å and 2.87 Å as maximal for **4 k**-COX-1 and **4 k**-COX-2, respectively; red, blue and interacted-residues in white areas of RMSF were obtained as expected, and all of them were very similar to previous studies [51,67–69]. These data show that the **4 k**-COXs' complexes are stable during simulation time and the results of interactions are reliable.

According to **D**, **E**, and **F** in Fig. 9 and **video1**, the interactions were very similar to docking poses, thus, their stability and strength were protected. Moreover, we did not observe a salt-bridge contact from the docking study, but it revealed that there is one with Arg120. On the other hand, water molecules have a positive impact on the stability because of forming water-mediated H-bonds with Arg120 (52 % and 63 %), Ser353 (29 % and 35 %), Pro514 (96 %), Leu352 (76 %), Asn515 (20 %) and Ser516 (80 %). In fact, we did not observe an interaction with Tyr348 and Ser353 according to the docking study, but the MDS study revealed that. These residues are a member of a loop region (seq. 347–362) like Tyr355, which plays a role with Arg120 and Glu524 in forming a constriction that must open to provide access into the active site. Therewithal, interactions with Tyr355 were insufficient to impact directly on stability in this case, but various interaction types were observed with this residue during the entire simulation time (Fig. 9**E**). Therefore, we think that interactions with Tyr348, Ser353 and Tyr355 are involved together to stabilize this loop region of the enzyme. So, *N, N*-dithiazole, and 2-nitrophenyl moieties play an important role in binding to constriction residues of the enzyme. On the other hand, even COX-1 side pocket is smaller than COX-2's, **4 k** can bind to His90, His513, Pro514, and Asn515 residues via its carboxylic acid.

According to **D**, **E**, and **F** in Fig. 10 and **video2**, interactions with Arg120 and Tyr355 residues were continuous during simulation time, however, interactions with Tyr355 were mostly hydrophobic and

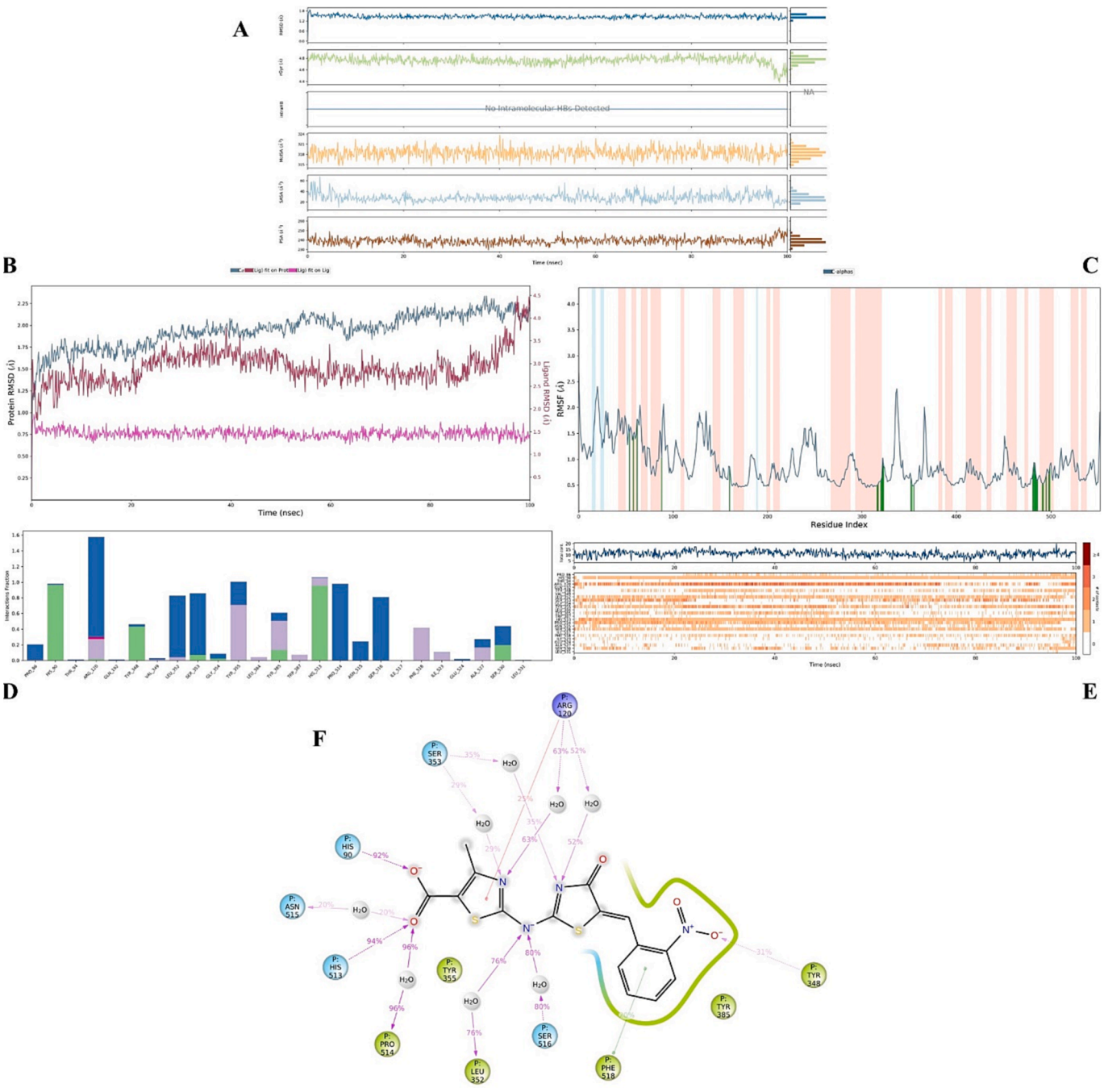

Fig. 9. MDS results **4 k**-COX-1 complex.

sometimes observed as water-mediated H-bond, thus it was insufficient to stabilize the enzyme complex in contrast to interactions with Arg120. However, we suggest that it has a positive impact on inhibitory activity through hydrophobic interactions. Briefly, **4 k** has interacted with constricted loop residues continuously during the entire simulation, which is vital to observe COX inhibition activity. On the other hand, the interactions with Phe518 were mostly hydrophobic, even though they were continuous, in comparison with the interactions of Phe518 of COX-1, interactions of COX-2′s Phe518 were observed not powerful. **4 k** interacted more stable with the side pocket of COX-2 than COX-1′s. The reason of that probably depends on the volume of the side pocket (His90, Thr94, and Arg513 of COX-2). So, we precipitated that this small acidic moiety (carboxylic acid) on thiazole is resulting inhibitory effect on both COX isoenzymes while it is more effective against COX-2. However, to determine this difference absolutely, we need advanced *in vivo* tests, or to compare bulky acidic groups. In fact, as reported in previous studies [51,70,71], when this acidic moiety was a bulky group such as sulfonyl amide, then it showed selectivity on COX-2 enzyme, and so these studies propounded the same insight. Briefly, an acidic group is a very important feature to observe COX inhibition, and also it plays a role in the determination of selectivity. Meanwhile, interactions with Tyr385 of COX-2 were stronger and, thereof, more stable than COX-1′s Tyr385 because of similar reasons to interactions with Phe518 residue.

The findings of *in silico* studies strongly supported the pharmacological data, revealing strong interactions of effective compounds with target proteins. On the other hand, in order for the analogs shown to be effective in this study to gain value as drugs, their safety must first be proven, and their clinical efficacy must be tested in patients with painful

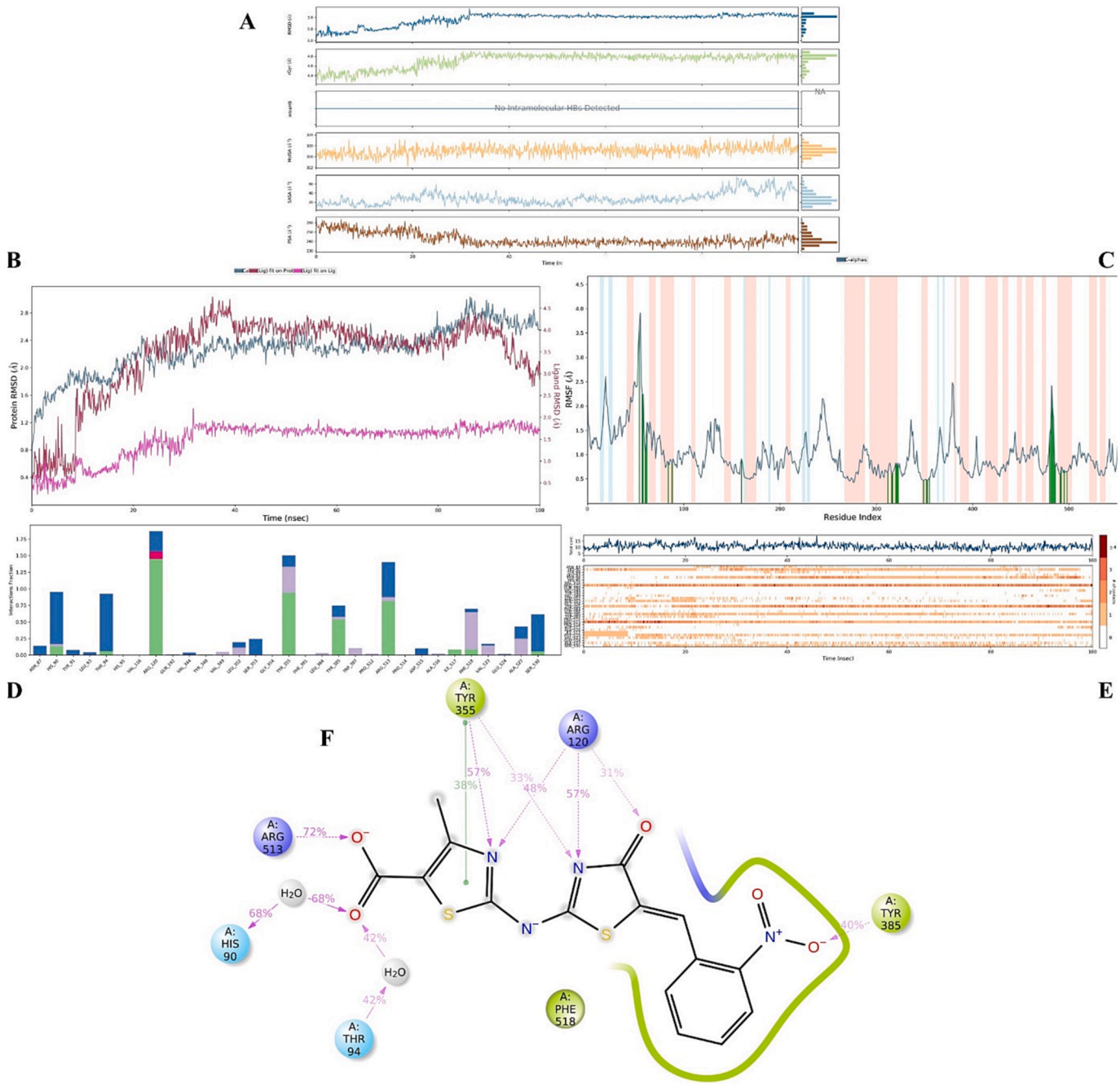

Fig. 10. MDS results **4 k**-COX-2 complex.

inflammatory disease. Additionally, *N,N*-dithiazole hybridization was found very effective, because its heteroatoms can interact directly or water-mediated with constricted loop region, especially when this core has an acidic group or feature, then the COX inhibition activity increases and the selectivity on COX isoenzymes can be managed.

Briefly, *in silico* and *in vitro* studies suggested together that the mechanism of action was related to COX inhibition. However, to make it certain, *in vitro* COX inhibition studies may be considered.

Because this new pharmacophore structure, which is an alternative to aryl acetic/propionic acid drugs, is opening a new area for discovering new anti-inflammatory and analgesic agents, this study gives new and alternative opportunities to medicinal chemists for the development of new and effective NSAIs.

5. Conclusion

In this study, based on the need of new anti-inflammatory and analgesic drugs with increased effectiveness and safer side effect profiles, we designed and synthesized some novel dithiazole carboxylic acid derivatives. For this purpose eleven novel *N,N*-dithiazole amine molecules including carboxylic acid and chalcone functional groups were synthesized via four steps and then their molecular structures analyzed by HRMS and NMR techniques. Possible anti-inflammatory and analgesic activities of these compounds were evaluated by various reliable *in vivo* tests. Pharmacological findings revealed that none of the derivatives was effective in the hot-plate or tail-clip tests, suggesting that they were ineffective on central pain mechanisms. On the other hand, it was observed that compounds **4b, 4c**, **4f**, **4 h,** and **4 k** in the series shortened the paw licking time of mice in the late phase of the formalin test, and

this finding indicated the peripherally-mediated antinociceptive effects of the compounds. The same compounds, besides, showed potent anti-inflammatory activities by significantly reducing paw edema of rats in the inflammation tests. Moreover, our *in silico* studies showed that both COX isoenzymes have important roles in the anti-inflammatory and analgesic activities of compounds **4b, 4c**, **4f**, **4 h,** and **4 k**. In conclusion, the findings of this multidisciplinary study investigating the design, synthesis, pharmacokinetic screening, pharmacological activity and molecular interaction properties of some new dithiazole carboxylic acid derivatives indicate that compounds **4b, 4c**, **4f**, **4 h,** and **4 k** have significant potentials as anti-inflammatory and analgesic drug candidates.

CRediT authorship contribution statement

Nazlı Turan Yücel: Data curation, Formal analysis, Investigation, Writing – original draft. **Abd Al Rahman Asfour:** Data curation, Formal analysis, Investigation, Writing – original draft. **Asaf Evrim Evren:** Conceptualization, Formal analysis, Investigation, Methodology, Project administration, Software, Writing – original draft, Writing – review & editing, Visualization. **Cevşen Yazıcı:** Data curation, Investigation, Methodology. **Ümmühan Kandemir:** Data curation, Investigation, Methodology. **Ümide Demir Özkay:** Conceptualization, Data curation, Formal analysis, Investigation, Supervision, Writing – original draft, Writing – review & editing. **Özgür Devrim Can:** Conceptualization, Data curation, Formal analysis, Investigation, Supervision, Writing – original draft, Writing – review & editing. **Leyla Yurttaş:** Conceptualization, Data curation, Formal analysis, Resources, Supervision, Visualization, Writing – original draft, Writing – review & editing.

Declaration of competing interest

The authors declare that they have no known competing financial interests or personal relationships that could have appeared to influence the work reported in this paper.

Acknowledgement

The authors present their gratitude to MERLAB and Anadolu University. All analyzed data were shared in the supplementary file and MDS videos were stored as supplementary files.

Appendix A. Supplementary data

Supplementary data to this article can be found online at https://doi.org/10.1016/j.bioorg.2024.107120.

References

[1] A.U. Tatiya, A.K. Saluja, M.G. Kalaskar, S.J. Surana, P.H. Patil, Evaluation of analgesic and anti-inflammatory activity of Bridelia retusa (Spreng) bark, J. Tradit. Complement. Med. 7 (4) (2017) 441–451.
[2] X. Zhang, V. Retyunskiy, S. Qiao, Y. Zhao, C.-M. Tzeng, Alloferon-1 ameliorates acute inflammatory responses in λ-carrageenan-induced paw edema in mice, Sci Rep 12 (1) (2022) 16689.
[3] J.H. Choi, D.S. Cha, H. Jeon, Anti-inflammatory and anti-nociceptive properties of Prunus padus, J. Ethnopharmacol. 144 (2) (2012) 379–386.
[4] V.C. Wang, W.J. Mullally, Pain neurology, Am. J. Med. 133 (3) (2020) 273–280.
[5] M. Al Malyan, C. Becchi, S. Boncinelli, N. Ashammakhi, Novel drug delivery systems in pain therapy, Minerva Anestesiol. 73 (3) (2006) 173–179.
[6] D. Hadjipavlou-Litina, Quantitative structure–activity relationship (QSAR) studies on non steroidal anti-inflammatory drugs (NSAIDs), Curr Med Chem 7 (4) (2000) 375–388.
[7] C. Mikra, G. Rossos, S.K. Hadjikakou, N. Kourkoumelis, Molecular docking and structure activity relationship studies of NSAIDs. what do they reveal about IC50? Lett Drug Des Discov 14 (8) (2017).
[8] F. Pehourcq, M. Matoga, B. Bannwarth, Diffusion of arylpropionate non-steroidal anti-inflammatory drugs into the cerebrospinal fluid: a quantitative structure-activity relationship approach, Fundam Clin Pharmacol 18 (1) (2004) 65–70.
[9] V.F. Roche, A receptor-grounded approach to teaching nonsteroidal antiinflammatory drug chemistry and structure-activity relationships, Am J Pharm Educ 73 (8) (2009) 143.
[10] M.J. Uddin, B.C. Crews, K. Ghebreselasie, L.J. Marnett, Design, synthesis, and structure–activity relationship studies of fluorescent inhibitors of cycloxygenase-2 as targeted optical imaging agents, Bioconjug. Chem. 24 (4) (2013) 712–723.
[11] A. Zarghi, S. Arfaei, Selective COX-2 inhibitors: a review of their structure-activity relationships, Iranian Journal of Pharmaceutical Research: IJPR 10 (4) (2011) 655.
[12] S. Bala, S. Kamboj, V. Saini, D.N. Prasad, Anti-inflammatory, analgesic evaluation and molecular docking studies of n-phenyl anthranilic acid-based 1,3,4-oxadiazole analogues, J. Chem. 2013 (2013) 1–6.
[13] A.A. Elhenawy, L.M. Al-Harbi, G.O. Moustafa, M.A. El-Gazzar, R.F. Abdel-Rahman, A.E. Salim, Synthesis, comparative docking, and pharmacological activity of naproxen amino acid derivatives as possible anti-inflammatory and analgesic agents, Drug Des Devel Ther 13 (2019) 1773–1790.
[14] S. Gotoh, J. Onaya, M. Abe, K. Miyazaki, A. Hamai, K. Horie, K. Tokuyasu, Effects of the molecular weight of hyaluronic acid and its action mechanisms on experimental joint pain in rats, Ann Rheum Dis 52 (11) (1993) 817–822.
[15] M.S. Hussain, F. Azam, H.A. Eldarrat, I. Alkskas, J.A. Mayoof, J.M. Dammona, H. Ismail, M. Ali, M. Arif, A. Haque, Anti-inflammatory, analgesic and molecular docking studies of Lanostanoic acid 3-O-α-D-glycopyranoside isolated from Helichrysum stoechas, Arabian J. Chem. 13 (12) (2020) 9196–9206.
[16] D.S. Krivokolysko, V.V. Dotsenko, E.Y. Bibik, A.A. Samokish, Y.S. Venidiktova, K. A. Frolov, S.G. Krivokolysko, A.A. Pankov, N.A. Aksenov, I.V. Aksenova, New hybrid molecules based on sulfur-containing nicotinonitriles: synthesis, analgesic activity in acetic acid-induced writhing test, and molecular docking studies, Russian Journal of Bioorganic Chemistry 48 (3) (2022) 628–635.
[17] A.E. Evren, A.B. Karaduman, B.N. Saglik, Y. Ozkay, L. Yurttas, Investigation of novel quinoline-thiazole derivatives as antimicrobial agents In Vitro and in Silico Approaches, ACS Omega 8 (1) (2023) 1410–1429.
[18] D. Nuha, A.E. Evren, Ö. Kapusiz, Ü.D. Gül, N. Gundogdu-Karaburun, A. Ç. Karaburun, H. Berber, Design, synthesis, and antimicrobial activity of novel coumarin derivatives: an in-silico and in-vitro study, J Mol Struct 1272 (2023) 134166.
[19] R.H.H. Salih, A.H. Hasan, N.H. Hussen, F.E. Hawaiz, T.B. Hadda, J. Jamalis, F. A. Almalki, A.S. Adeyinka, L.-C.-C. Coetzee, A.K. Oyebamiji, Thiazole-pyrazoline hybrids as potential antimicrobial agent: Synthesis, biological evaluation, molecular docking, DFT Studies and POM Analysis, J Mol Struct 1282 (2023) 135191.
[20] F. Başoğlu-ünal, S. Cimok, E.D. DİNCEL, L. Naesens, N. Ulusoy-Güzeldemirci, Novel 4-thiazolidinone derivatives bearing imidazo [2, 1-b] thiazole moiety: design, synthesis, and antiviral activity evaluation, Journal of Research in Pharmacy 27 (2) (2023).
[21] P. venkatesham, D. Schols, L. Persoons, S. Claes, A.A. Sangolkar, R. Chedupaka, R. R. Vedula, Synthesis of novel thioalkylated triazolothiazoles and their promising in-vitro antiviral activity, J Mol Struct (2023, 1286,) 135573.
[22] G.H. Alfaifi, T.A. Farghaly, H.A. Magda, Indenyl-thiazole and indenyl-formazan derivatives: synthesis, anticancer screening studies, molecular-docking, and pharmacokinetic/ molin-spiration properties, PLoS One 18 (3) (2023) e0274459.
[23] A.E. Evren, D. Nuha, L. Yurttaş, Focusing on the moderately active compound (MAC) in the design and development of strategies to optimize the apoptotic effect by molecular mechanics techniques, European Journal of Life Sciences 1 (3) (2022) 118–126.
[24] A.E. Evren, D. Nuha, S. Dawbaa, A.B. Karaduman, B.N. Saglik, L. Yurttas, Novel oxadiazole-thiadiazole derivatives: synthesis, biological evaluation, and in silico studies, J Biomol Struct Dyn (2023) 1–13.
[25] H. Aziz, A. Saeed, C.J. McAdam, J. Simpson, T. Hökelek, E. Jabeen, A. Khurshid, M. Saleem, H.R. El-Seedi, Synthesis, single crystal structure determinations, Hirshfeld surface analysis, crystal voids, interaction energies, and density functional theory studies of functionalized 1,3-thiazoles, J Mol Struct 1281 (2023) 135108.
[26] A. Markovic, A. Zivkovic, M. Atanasova, I. Doytchinova, B. Hofmann, S. George, S. Kretschmer, C. Rodl, D. Steinhilber, H. Stark, A. Smelcerovic, Thiazole derivatives as dual inhibitors of deoxyribonuclease I and 5-lipoxygenase: a promising scaffold for the development of neuroprotective drugs, Chem Biol Interact 381 (2023) 110542.
[27] Y. Yang, N. Wang, L. Xu, Y. Liu, L. Huang, M. Gu, Y. Wu, W. Guo, H. Sun, Aryl hydrocarbon receptor dependent anti-inflammation and neuroprotective effects of tryptophan metabolites on retinal ischemia/reperfusion injury, Cell Death Dis 14 (2) (2023) 92.
[28] G.L. Khatik, A.K. Datusalia, W. Ahsan, P. Kaur, M. Vyas, A. Mittal, S.K. Nayak, A retrospect study on thiazole derivatives as the potential antidiabetic agents in drug discovery and developments, Curr Drug Discov Technol 15 (3) (2018) 163–177.
[29] Z. Li, Q. Qiu, X. Xu, X. Wang, L. Jiao, X. Su, M. Pan, W. Huang, H. Qian, Design, synthesis and Structure-activity relationship studies of new thiazole-based free fatty acid receptor 1 agonists for the treatment of type 2 diabetes, Eur. J. Med. Chem. 113 (2016) 246–257.
[30] A.K. Mohammed Iqbal, A.Y. Khan, M.B. Kalashetti, N.S. Belavagi, Y.D. Gong, I. A. Khazi, Synthesis, hypoglycemic and hypolipidemic activities of novel thiazolidinedione derivatives containing thiazole/triazole/oxadiazole ring, Eur. J. Med. Chem. 53 (1) (2012) 308–315.
[31] R.G. Kalkhambkar, G.M. Kulkarni, H. Shivkumar, R.N. Rao, Synthesis of novel triheterocyclic thiazoles as anti-inflammatory and analgesic agents, Eur. J. Med. Chem. 42 (10) (2007) 1272–1276.
[32] H. Karaca Gençer, Tiyazol-fenilasetik asit bileşiklerinin dual antibakteriyel-COX enzim inhibitörleri olarak sentezleri, Cukurova Medical Journal (çukurova Üniversitesi Tıp Fakültesi Dergisi) 42 (4) (2017) 1.

[33] G. Kumar, N.P. Singh, Synthesis, anti-inflammatory and analgesic evaluation of thiazole/oxazole substituted benzothiazole derivatives, Bioorg Chem 107 (2021) 104608.
[34] Z.Y. Fu, Q.H. Jin, Y.L. Qu, L.P. Guan, Chalcone derivatives bearing chromen or benzo[f]chromen moieties: design, synthesis, and evaluations of anti-inflammatory, analgesic, selective COX-2 inhibitory activities, Bioorg Med Chem Lett 29 (15) (2019) 1909–1912.
[35] J. Higgs, C. Wasowski, A. Marcos, M. Jukic, C.H. Pavan, S. Gobec, F. de Tezanos Pinto, N. Colettis, M. Marder, Chalcone derivatives: synthesis, in vitro and in vivo evaluation of their anti-anxiety, anti-depression and analgesic effects, Heliyon 5 (3) (2019) e01376.
[36] Z.H. Huang, L.Q. Yin, L.P. Guan, Z.H. Li, C. Tan, Screening of chalcone analogs with anti-depressant, anti-inflammatory, analgesic, and COX-2-inhibiting effects, Bioorg Med Chem Lett 30 (11) (2020) 127173.
[37] G.S. Viana, M.A. Bandeira, F.J. Matos, Analgesic and antiinflammatory effects of chalcones isolated from Myracrodruon urundeuva allemao, Phytomedicine 10 (2–3) (2003) 189–195.
[38] S.M. El-Messery, G.S. Hassan, F.A. Al-Omary, H.I. El-Subbagh, Substituted thiazoles VI. Synthesis and antitumor activity of new 2-acetamido- and 2 or 3-propanamido-thiazole analogs, Eur. J. Med. Chem. 54 (2012) 615–625.
[39] M.F. Abo-Ashour, W.M. Eldehna, R.F. George, M.M. Abdel-Aziz, M.M. Elaasser, N. M. Abdel Gawad, A. Gupta, S. Bhakta, S.M. Abou-Seri, Novel indole-thiazolidinone conjugates: design, synthesis and whole-cell phenotypic evaluation as a novel class of antimicrobial agents, Eur. J. Med. Chem. 160 (2018) 49–60.
[40] M.M. Amin, M.R. Shaaban, N.T. Al-Qurashi, H.K. Mahmoud, T.A. Farghaly, Indomethacin analogs: synthesis, anti-inflammatory and analgesic activities of indoline derivatives, Mini Rev Med Chem 18 (16) (2018) 1409–1421.
[41] N. Turan Yücel, Ü. Kandemir, Ü. Demir Özkay, Ö.D. Can, 5-HT1A Serotonergic, α-adrenergic and opioidergic receptors mediate the analgesic efficacy of vortioxetine in mice, Molecules 26 (11) (2021) 3242.
[42] M. Ratheesh, G. Sindhu, A. Helen, Anti-inflammatory effect of quinoline alkaloid skimmianine isolated from Ruta graveolens L, Inflammation Res. 62 (2013) 367–376.
[43] Ö. Güzelad, A. Özkan, H. Parlak, O. Sinen, E. Afşar, E. Öğüt, F.B. Yıldırım, M. Bülbül, A. Ağar, M. Aslan, Protective mechanism of Syringic acid in an experimental model of Parkinson's disease, Metab. Brain Dis. 36 (2021) 1003–1014.
[44] M. Kasap, Ö.D. Can, Opioid system mediated anti-nociceptive effect of agomelatine in mice, Life Sci. 163 (2016) 55–63.
[45] N.T. Yucel, D. Osmaniye, U. Kandemir, A.E. Evren, O.D. Can, U. Demir Ozkay, Synthesis and antinociceptive effect of some thiazole-piperazine derivatives: involvement of opioidergic system in the activity, Molecules 26 (11) (2021).
[46] U. Demir Ozkay, O.D. Can, Anti-nociceptive effect of vitexin mediated by the opioid system in mice, Pharmacol Biochem Behav 109 (2013) 23–30.
[47] S. Yano, Y. Suzuki, M. Yuzurihara, Y. Kase, S. Takeda, S. Watanabe, M. Aburada, K.-I. Miyamoto, Antinociceptive effect of methyleugenol on formalin-induced hyperalgesia in mice, Eur. J. Pharmacol. 553 (1–3) (2006) 99–103.
[48] W. Ridtitid, C. Sae-Wong, W. Reanmongkol, M. Wongnawa, Antinociceptive activity of the methanolic extract of Kaempferia galanga Linn. in experimental animals, J. Ethnopharmacol. 118 (2) (2008) 225–230.
[49] H. Sadeghi, V. Hajhashemi, M. Minaiyan, A. Movahedian, A. Talebi, A study on the mechanisms involving the anti-inflammatory effect of amitriptyline in carrageenan-induced paw edema in rats, Eur J Pharmacol 667 (1–3) (2011) 396–401.
[50] A. Avci, H. Tasci, U. Kandemir, O.D. Can, N. Gokhan-Kelekci, B. Tozkoparan, Synthesis, characterization, and in vivo pharmacological evaluation of novel mannich bases derived from 1,2,4-triazole containing a naproxen moiety, Bioorg Chem 100 (2020) 103892.
[51] D. Osmaniye, A.E. Evren, Ş. Karaca, Y. Özkay, Z.A. Kaplancıklı, Novel thiadiazol derivatives; design, synthesis, biological activity, molecular docking and molecular dynamics, J Mol Struct 1272 (2023) 134171.
[52] E. Guzel, U. Acar Cevik, A.E. Evren, H.E. Bostanci, U.D. Gul, U. Kayis, Y. Ozkay, Z. A. Kaplancikli, Synthesis of benzimidazole-1,2,4-triazole derivatives as potential antifungal agents targeting 14alpha-demethylase, ACS Omega 8 (4) (2023) 4369–4384.
[53] S. Dawbaa, D. Nuha, A.E. Evren, M.Y. Cankiliç, L. Yurttaş, G. Turan, New oxadiazole/triazole derivatives with antimicrobial and antioxidant properties, J Mol Struct 1282 (2023) 135213.
[54] A.A. Al-Sharabi, S. Saffour, A.E. Evren, G. Bayazıt, G. Çongur, Ü.D. Gül, L. Yurttaş, Synthesis, antimicrobial activity, electrochemical studies and molecular modeling studies of novel 1,3,4-oxadiazole derivatives, J Mol Struct 1289 (2023) 135775.
[55] Schrödinger Release 2020-3, Maestro, Schrödinger, LLC, New York, NY, USA, 2020.
[56] Schrödinger release. 2020-3: LigPrep 2020, Schrödinger, LLC, New York, NY, USA, 2020.
[57] Schrödinger Release 2020-3, Glide, Schrödinger, LLC, New York, NY, USA, 2020.
[58] S.A. Naji, B.N. Sağlik, M. Agamennone, A.E. Evren, N. Gundogdu-Karaburun, A. Ç. Karaburun, Design and evaluation of synthesized pyrrole derivatives as dual COX-1 and COX-2 inhibitors using FB-QSAR approach, ACS Omega (2023).
[59] Schrödinger Release 2020-3, Desmond, Schrödinger, LLC, New York, NY, USA, 2020.
[60] D. Le Bars, M. Gozariu, S.W. Cadden, Animal models of nociception, Pharmacol. Rev. 53 (4) (2001) 597–652.
[61] J.R. Deuis, L.S. Dvorakova, I. Vetter, Methods used to evaluate pain behaviors in rodents, Front. Mol. Neurosci. 10 (2017) 284.
[62] S. Hunskaar, K. Hole, The formalin test in mice: dissociation between inflammatory and non-inflammatory pain, Pain 30 (1) (1987) 103–114.
[63] A. Tjølsen, O.-G. Berge, S. Hunskaar, J.H. Rosland, K. Hole, The formalin test: an evaluation of the method, Pain 51 (1) (1992) 5–17.
[64] S. Islam, M.S. Shajib, R.B. Rashid, M.F. Khan, M.A. Al-Mansur, B.K. Datta, M. A. Rashid, Antinociceptive activities of Artocarpus lacucha Buch-ham (Moraceae) and its isolated phenolic compound, catechin, in mice, BMC Complement. Altern. Med. 19 (1) (2019) 1–13.
[65] M.N.U. Chy, M. Adnan, M.R. Chowdhury, E. Pagano, A.M. Kamal, K.K. Oh, D. H. Cho, R. Capasso, Central and peripheral pain intervention by Ophiorrhiza rugosa leaves: potential underlying mechanisms and insight into the role of pain modulators, J. Ethnopharmacol. 276 (2021) 114182.
[66] M. Di Rosa, Biological properties of carrageenan, J. Pharm. Pharmacol. 24 (2) (1972) 89–102.
[67] S.A. Ganai, S. Rajamanikandan, B.A. Shah, A. Lone, F. Arwa, F.A. Malik, Comparative structural study of selective and non-selective NSAIDs against the enzyme cyclooxygenase-2 through real-time molecular dynamics linked to post-dynamics MM-GBSA and e-pharmacophores mapping, J Mol Model 29 (6) (2023) 192.
[68] M.M. Sabry, R.F. Abdel-Rahman, H.M. Fayed, A.T. Taher, H.A. Ogaly, A. Albohy, S. H. El-Gayed, R.M. Ibrahim, Impact of Eucalyptus maculata Hook resin exudate constituents on reducing COX-2 gene expression: in-vivo anti-inflammatory, molecular docking and dynamics studies, J Ethnopharmacol 314 (2023) 116631.
[69] M. Yadav, M. Abdalla, M. Madhavi, I. Chopra, A. Bhrdwaj, L. Soni, U. Shaheen, L. Prajapati, M. Sharma, M.S. Sikarwar, S. Albogami, T. Hussain, A. Nayarisseri, S. K. Singh, Structure-based virtual screening, molecular docking, molecular dynamics simulation and pharmacokinetic modelling of cyclooxygenase-2 (COX-2) inhibitor for the clinical treatment of colorectal cancer, Mol. Simul. 48 (12) (2022) 1081–1101.
[70] V.T. Angelova, T. Tatarova, R. Mihaylova, N. Vassilev, B. Petrov, Z. Zhivkova, I. Doytchinova, Novel arylsulfonylhydrazones as breast anticancer agents discovered by quantitative structure-activity relationships, Molecules 28 (5) (2023).
[71] J. Mikus, P. Swiatek, P. Przybyla, E. Krzyzak, A. Marciniak, A. Kotynia, A. Redzicka, B. Wiatrak, P. Jawien, T. Gebarowski, L. Szczukowski, Synthesis, biological, spectroscopic and computational investigations of novel N-acylhydrazone derivatives of pyrrolo[3,4-d]pyridazinone as dual COX/LOX inhibitors, Molecules 28 (14) (2023).